Classification
Physics Abstracts
61.16D — 61.60

HREM studies of complex uranium oxides containing molybdenum and tungsten

Margareta Sundberg([1]) and Valeri Tabachenko([2])

([1]) Department of Inorganic Chemistry, Arrhenius Laboratory, Stockholm University, S-10691 Stockholm, Sweden

([2]) X-ray Laboratory, Department of Inorganic Chemistry, Faculty of Chemistry, Moscow State University, U.S.S.R.

(Received October 29, 1990; accepted January 04, 1991)

Résumé. — La microscopie haute résolution, la diffraction X sur poudres et sur monocristal ont été utilisées pour caractériser les phases formées par réactions à l'état solide dans le systeme UO_2 – MoO_2 – MoO_3 – WO_3. Quelques phases sont décrites comme des membres d'une série homologue construite avec des feuillets de différentes épaisseurs de type ReO_3. D'après les résultats antérieurs en diffraction X, ces feuillets sont connectés par des atomes U et O de telle sorte que de fins feuillets plissés de bipyramides pentagonales UO_7, reliées par des arêtes, sont formés. La formule générale est $UO \cdot M_nO_{3n+1}$, n est le nombre d'octaèdres selon un feuillet ReO_3. Des structures formées de feuillets de type ReO_3 ordonné et de largeur n =2, 4 et 5 ont été examinés. De manière similaire, cet ensemble de phases peut être considéré comme une intercroissance de structure de type UVO_5 avec les feuillets ReO_3 de différentes épaisseurs. Dans les phases pour lesquelles U est remplacé par Mo ou W, les feuillets ReO_3 sont connectés par des octaèdres MoO_6 de telle sorte que des tunnels à 6 côtés sont formés et dans lesquels existent des chaines d'atomes -O -U -O -U. Enfin, un arrangement presque ordonné de bipyramides hexagonales UO_8 et d'octaèdres ReO_3 connecte les feuillets ReO_3. La formule générale pour cette série homologue est $U_{1-x}\square_x O \cdot mMO_3$, où $\square$ est une lacune et $m = 2n+1$ (n : nombre d'octaèdres MO_6 formant le feuillet ReO_3). Le réseau base de ces structures peut être considéré comme l'intercroissance de feuillets de type HTB (Bronze de Tungstène hexagonal), d'une rangée de tunnels vides avec les feuillets ReO_3 d'épaisseurs différentes. Les phases construites à partir de feuillets ReO_3 avec n = 3, 4 et 5 et avec une occupation moitié des atomes U (x = 0, 5) dans les tunnels à 6 côtés ont été étudiées, de même que UMo_5O_{16} dont l'occupation des positions U est complète avec les feuillets ReO_3 de 2 octaèdres d'épaisseur. La structure $U_{0,5}(Mo, W)_9O_{28}$ possède un ordre sur les lacunes. Cette série est voisine des structures d'intercroissance de Bronzes de Tungstene (ITB).

Abstract. — HREM, X-ray powder and single-crystal diffraction techniques were used to characterize phases formed in the UO_2 – MoO_2 – MoO_3 – WO_3 system by solid state reaction. Some of the phases studied can be described as members of a homologous series of structures built up of ReO_3– type slabs of different widths. According to previous X-ray studies, these slabs are connected by U and O atoms so that thin pleated slabs of edge sharing pentagonal UO_7– bipyramids are formed. The general formula is $UO \cdot M_nO_{3n+1}$, where n = number of octahedra across the ReO_3– type slab. Structures containing ordered ReO_3– type slabs of n =2, 4 and 5 widths have been examined. Alternatively, this set of phases can be regarded as intergrowths of an UVO_5– type structure with ReO_3– type slabs of different widths. In phases where U is replaced by Mo or W, the ReO_3– type slabs are connected by MoO_6– octahedra so that six-sided tunnels are formed, in which strings of -O-U-O-U-

atoms are found. Hence, an almost planar ordered arrangement of hexagonal UO_8- bipyramids and MoO_6- octahedra connects the ReO_3- type slabs. The general formula of this homologous series of phases is $U_{1-x}\square_x O \cdot mMO_3$, where $\square$ = vacancy and $m = 2n+1$ (n = number of MO_6- octahedra across the ReO_3- type slab). The basic network structure can be considered as an intergrowth of slabs of HTB- elements (hexagonal tungsten bronze), one tunnel row wide, with ReO_3- type slabs of different widths. Phases built up of ReO_3- type slabs with n =3, 4 and 5 with half occupancy of U atoms ($x = 0.5$) in the six-sided tunnels have been studied, as well as UMo_5O_{16} with full occupancy of all U positions and with ReO_3-type slabs two octahedra wide. The $U_{0.5}(Mo, W)_9 O_{28}$ structure contained ordered vacancies. This series is closely related to the intergrowth tungsten bronze (ITB) structures.

1. Introduction.

Previous X-ray studies of complex uranium molybdenum oxides [1-6], have shown that a series of phases related to the orthorhombic $\beta - UMo_2O_8$ structure can be prepared. The structures can be described as built up of corner-sharing MO_6-octahedra that form slabs of ReO_3-type. The slabs extend indefinitely in two dimensions, while the width of the slabs is finite but variable. In the $\beta - UMo_2O_8$ structure [7] (Fig. 1a) the width of the ReO_3-type slab corresponds to two MO_6- octahedra. The slabs are mutually linked by -U-O-U-O- strings parallel to the short $c-$axis, of the structure so that cornersharing pentagonal UO_7-bipyramids are formed. Along the b = axis, the slabs can be described as linked by pleated edge-sharing chains of pentagonal UO_7- bipyramids. The unit cell dimensions given by Cremers *et al.* [7] are: a =20.076, b =7.323, c =4.1164 Å.

Partial substitution of molybdenum for uranium in $\beta - UMo_2O_8$ creates vacancies in the structure so as to maintain charge balance. Such substitutions have been made to form the $UMo_{10}O_{32}$ and $\alpha - U_3Mo_{20}O_{64}$ phases. X-ray structure determinations of these phases showed that vacancies were regularly distributed along the linkage plane between the ReO_3-type slabs. The $UMo_{10}O_{32}$ structure [5] is shown in figure 1b. As can be seen in figure 1, both structures consist of ReO_3-type slabs two MO_6-octahedra in width, but the atom arrangements between the slabs are different. In figure 1b, where the U atoms are partly replaced by Mo atoms and vacancies, MoO_6-octahedra connect the ReO_3-type slabs by cornersharing so that six-sided tunnels are formed, where strings of alternating U and O atoms can enter. The six-sided tunnels are thus transformed into rows of cornersharing hexagonal UO_8-bipyramids along the short crystal axis. In the $UMo_{10}O_{32}$ structure, only half of the available uranium positions are occupied by uranium atoms. The length of the $b-$axis in figure 1a is the same as that of the $c-$axis in figure 1b, while the $a-$axis in figure 1a is twice that in figure 1b.

High resolution electron microscopy (HREM) technique has previously been used to investigate order and disorder in a few complex oxide compounds, where U has been partly replaced by Mo and W. The structure models of UM_4O_{14} and UM_5O_{17}, where M = "W", have been derived from HREM images. These phases have been described as two members (n = 4 and n = 5) of the homologous series UM_nO_{3n+2}, M = "W" (8). The defect structures of "UW_5O_{17}" and $\gamma - U_3Mo_{20}O_{64}$ have also been examined by HREM technique [9].

The present investigation of the $UO_2 - MoO_2 - MoO_3 - WO_3$ system illustrates that a combination of different techniques is essential to establish detailed structures of the different phases formed. This present contribution, which is the first in a series of articles on complex uranium oxides, containing molybdenum and tungsten will report mainly on the electron microscopy studies of phases built up of ReO_3- type slabs of widths corresponding to two, three, four and five octahedra.

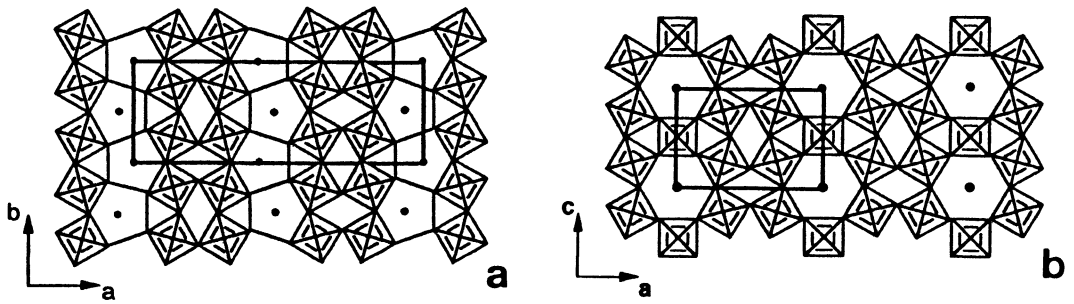

Fig. 1. — The idealized structures projected along the short crystal axis of a) β – UMo_2O_8 ([001] zone), b) UMo_5O_{16} ([010] zone). In the $UMo_{10}O_{32}$ structure, every tunnel is filled with strings of -O-U-O-U-, so that cornersharing hexagonal UO_8– bipyramids are formed, and every second tunnel is empty.

2. Experimental.

Samples of various compositions in different subsystems of the main system UO_2 – MoO_2– MoO_3– WO_3 were synthesised, by heating appropriate mixtures of binary oxides in evacuated silica tubes at 800-1000° C during 10-50 days, as will be described in detail elsewhere. Almost all samples obtained were multiphasic. Each specimen was examined optically and a few crystals of similar habitus and colour were selected for X-ray and electron microscopy studies.

X-ray powder photographs were taken in a focusing camera of Guinier-Hägg type, with monochromatized $CuK\alpha_1$ radiation and using Si as an internal standard. Powder patterns were recorded both of the bulk sample and of the selected crystals. The unit cell parameters were refined by least-squares techniques. Single-crystal X-ray diffraction studies were also made, but these results will be published separately.

The selected crystals were investigated by high-resolution transmission electron microscopy, electron diffraction and EDS techniques. All electron microscopy specimens were prepared by crushing the selected crystals in an agate mortar under n-butanol and allowing a drop of the suspension to dry of a holey carbon support film. The grids were examined in a JEOL 200CX electron microscope, equipped with top-entry goniometer stage allowing tilt angles of $\pm 10°$. The radius of the objective aperture used corresponded to 4.1 nm^{-1} in the reciprocal space. Theoretical images were calculated by using a local version of the SHRLI suite of programs [10]. A large number of fragments were also examined by electron diffraction in combination with EDS-analysis. This study was carried out with a JEOL 2000 FXII electron microscope, equipped with a LINK system.

3. Results.

a) UMo_5O_{16}.

A 50% substitution of U by Mo in β – UMo_2O_8 creates a phase UMo_5O_{16} in the subsystem UO_2 – MoO_2 – MoO_3. Selected crystals from a sample with the composition UO_2 : MoO_2 : MoO_3 =1:1:25 were of brown colour. Figure 2a shows a HREM image of a thin crystal fragment of the UMo_5O_{16} phase, recorded at a defocus value where the projected U and Mo atoms yield white contrast. The unit cell parameters, refined from X-ray powder data are a =9.9026 Å, b =4.1340 Å, c =7.1823 Å and β=90.20°. The length of the a–axis indicates a structure of the type shown in figure 1b, where all six-sided tunnels are filled with -U-O-U-O- strings so that rows of

cornersharing hexagonal UO_8–bipyramids are formed parallel to the b–axis. The stoichiometric composition of the model is UMo_5O_{16}.

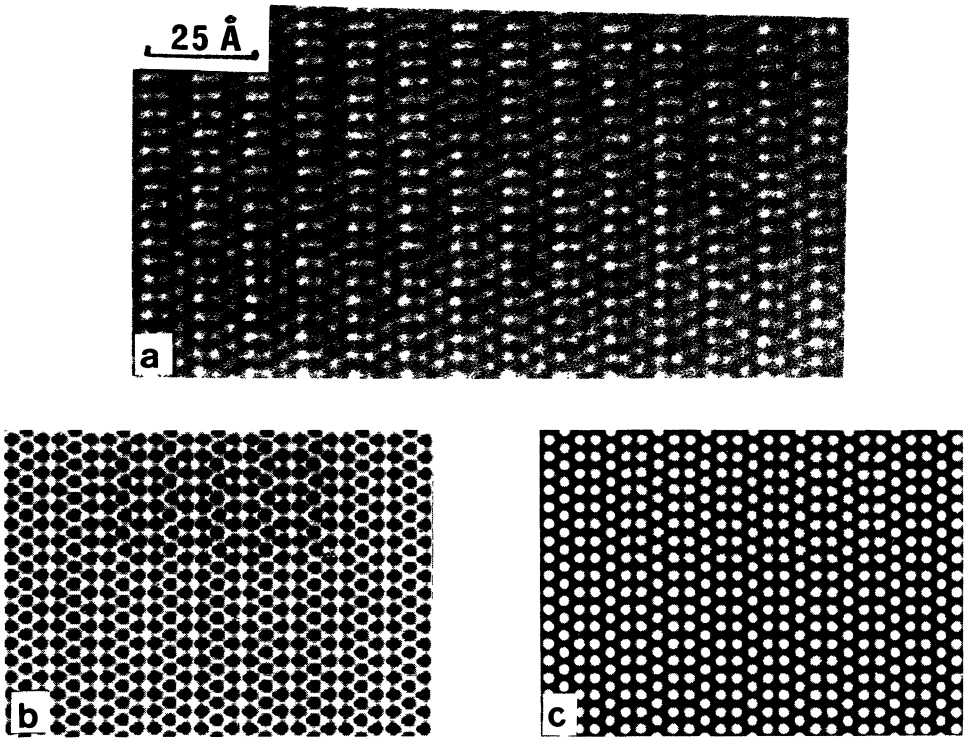

Fig. 2. — a) HREM image of UMo_5O_{16} projected along [010]. b,c) Calculated images of the UMo_5O_{16} structure with insets calculated for the β – UMo_2O_8 structure; (crystal thickness $\approx$20 Å), Defocus values; (b)–500. Å, (c)–900. Å. It is very hard to recognize the insets in these images, which shows that it is almost impossible to distinguish between these models from experimental images of thin crystals.

A set of calculated HREM images of the structure model in figure 1b, with full occupancy at all uranium and oxygen positions, is shown in figure 3a. The parameters used in the calculations were taken from the corresponding single-crystal X-ray study of the UMo_5O_{16} structure. Figure 3b illustrates a set of calculated images based on the parameters given by Cremers *et al.* [7] for the β – UMo_2O_8 structure. Both sets of images clearly demonstrate that the heavy metal atoms in projection are imaged as black spots in a small region of defocus values around –500 Å and with reversed contrast in a region arround –900 Å. For both cases the crystal thickness must be less than approximately 50 Å. For both structure models, there is good agreement between the experimental image in figure 2a and the calculated images for a defocus value of –900 Å. In figures 2b and 2c, the calculated image of β – UMo_2O_8 has been inserted into the corresponding calculated image of the UMo_5O_{16} structure model. These calculated images clearly show that for thin crystals (thickness <50 Å) it is impossible to distinguish between these two models without considering information obtained by other methods. On the other hand, the calculations show that for thicker crystals the images should be different. However, at larger thicknesses the contrast does not correspond to individual rows of heavy atoms, and the ReO_3–type pattern is not

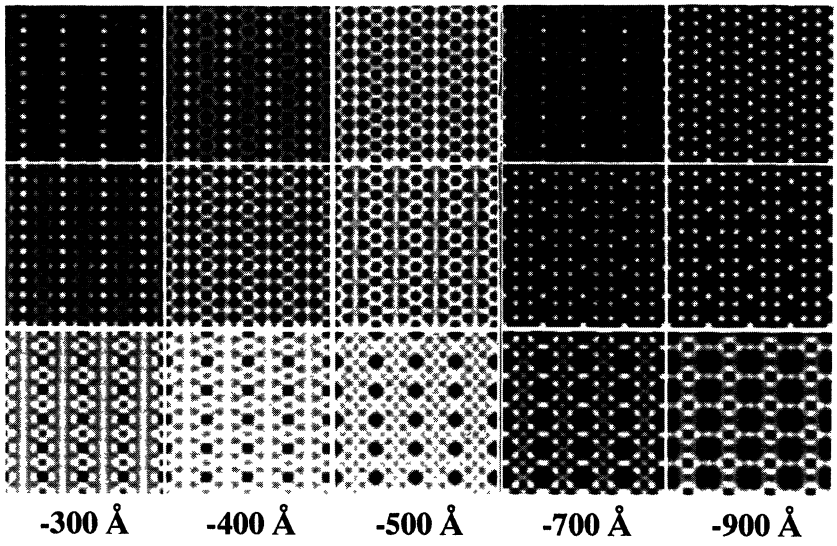

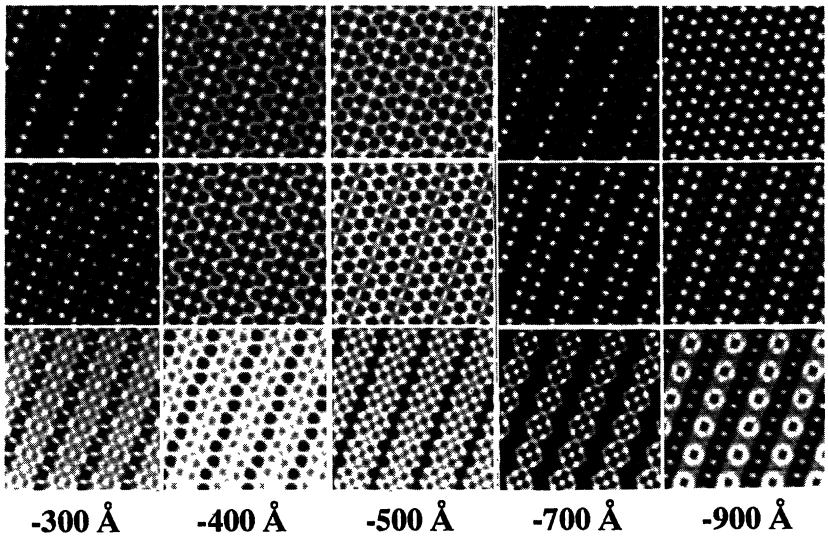

Fig. 3. — a) Simulated images of the UMo_5O_{16} structure. b) Simulated images of the $\beta - UMo_2O_8$ structure. Crystal thickness: first row 20 Å, middle row 40 Å, bottom row 60 Å. The defocus values are shown in the figure.

revealed, which makes a direct interpretation difficult. The contrast character in the micrograph of the thicker part of a fragment confirmed the UMo_5O_{16} models, however.

b)$U_{0.5}(Mo, W)_7O_{22}$.

Crystals of similar habitus and colour were selected from the bulk sample UO_2 : MoO_3 : WO_3 =1:7:4. The unit cell dimensions derived from the ED pattern taken along the short crystal

c–axis were $a \approx 27.1$ Å and $b \approx 7.2$ Å. Later, the unit cell parameters were refined from X-ray powder data and found to be $a = 27.227$ Å, $b = 7.2709$ Å and $c = 3.9766$ Å.

The contrast features in the HREM image (Fig. 4a) clearly indicate that the structure consists of slabs of ReO_3–type. The slabs are infinite in two dimensions and three octahedra wide.

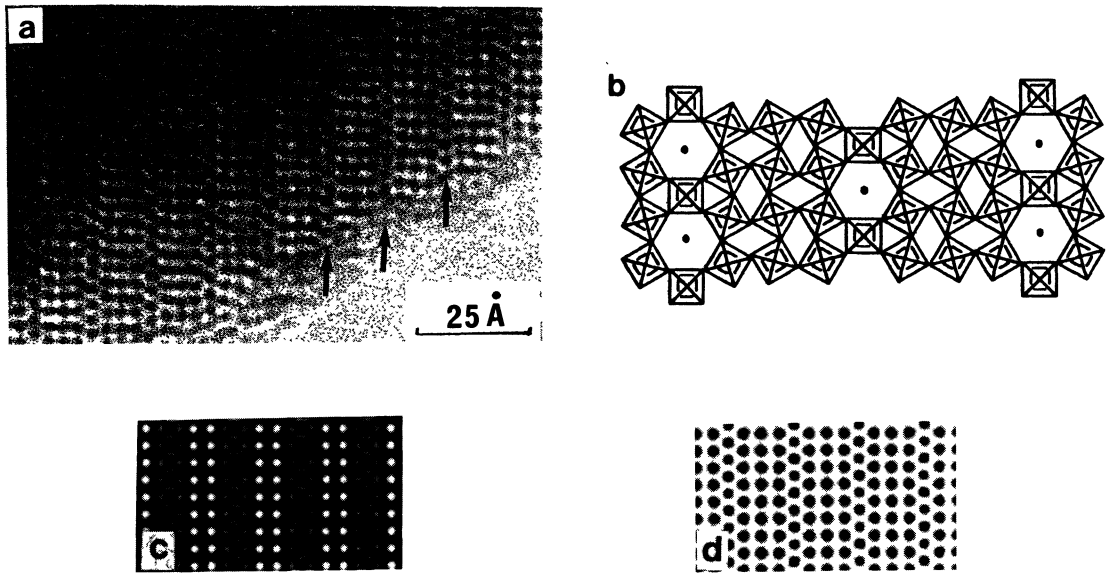

Fig. 4. — a) HREM image of a thin fragment of $U_{0.5}(Mo, W)_7O_{22}$; b) Idealized structure model of $U_{0.5}(Mo, W)_7O_{22}$; c,d) Calculated images of the model in (b), crystal thickness 20 Å, defocus values −400 Å (c), −500 Å (d).

The micrograph also shows almost straight lines of dark spots of uniform size and intensity between the ReO_3–type slabs (see arrows), making a straightforward interpretation of the contrast character difficult. The arrangement of dark spots can either be interpreted as an ordered arrangement of MoO_6– octahedra and hexagonal UO_8–bipyramids as in UMo_5O_{16} or as a zigzag chain of edge-sharing pentagonal UO_7–bipyramids such as existing in β – UMo_2O_8. The dimension of the a-axis and the contrast features in the HREM image suggest a structure such as that shown in figure 4b. With reference to the UMo_5O_{16} structure, it seems likely that the Mo/W-atoms occur in the MO_6–octahedra, while U- and O- atoms are located in the six-sided tunnels, so that hexagonal UO_8–bipyramids are formed. The network of corner-sharing MO_6– octahedra corresponds to a composition of $M_{14}O_{42}$, while full occupancy of the six-sided tunnels gives the composition $A_2M_{14}O_{44}$. In order to yield electroneutrality of the structure, the composition of the examined phase should be $U(Mo, W)_{14}O_{44}$, which means that only half of the hexagonal bipyramids are occupied by U-atoms. This U-content is also in agreement with EDS results obtained from ten different crystal fragments. The Mo/W ratio was found to be about 0.89 from the EDS measurements. The composition of this phase should thus be close to $U_{0.5}Mo_{3.3}W_{3.7}O_{22}$. The distributions of U atoms and vacancies seem to be random, as no superstructure reflexion has been observed in the ED patterns.

A single crystal X-ray investigation is under way. The results so far obtained verify the structure model shown in figure 4b. The central Mo and W atoms in the MO_6–octahedra seem to be displaced from the plane $z = 0$, so that a slightly puckerd arrangement of M- atoms in the

ReO_3–type slabs is obtained. Simulated HREM images of the structure model in figure 4b were calculated by using the atom positions obtained from the single-crystal x-ray study. There is good agreement between the observed image (Fig. 4a) and the calculated images (Figs.4c and 4d).

The $U_{0.5}Mo_{3.3}W_{3.7}O_{22}$ phase has not previously been observed in the $UO_2 - MoO_3 - WO_3$ system. All ED patterns recorded of thin crystal fragments indicated a well-ordered phase, as all reflexion spots were sharp and no streaking occurred. The HREM images showed exclusively ReO_3– type slabs three MO_6–octahedra wide. The image calculations showed that it is not possible to distinguish between the U and Mo atom positions in the linkage planes between the ReO_3–type slabs from the micrograph.

c) $U(Mo, W)_4O_{14}$ and $U_{0.5}(Mo, W)_{11}O_{34}$.

Electron microscopy studies of crystals selected from the bulk sample $UO_2 : MoO_3 : WO_3 =$ 1:3:11 yielded three distinct types of ED-pattern. Figure 5 illustrates that all these patterns are related to the same basic ReO_3–type structure but with slightly different unit cell parameters. The unit cell parameters were calculated to be $a \approx 2 \times 17.5 = 35.0$ Å, $b \approx 7.4$ Å, C-centered (Fig. 5a); $a \approx 2 \times 21.3 = 42.6$ Å, $b \approx 7.4$ Å C-centered (Fig. 5b) and $a \approx 21.3$ Å, $b \approx 7.4$ Å (Fig. 5c). Note the relationship between figures 5b and 5c; in figure 5b the a–axis is twice that in figure 5c.

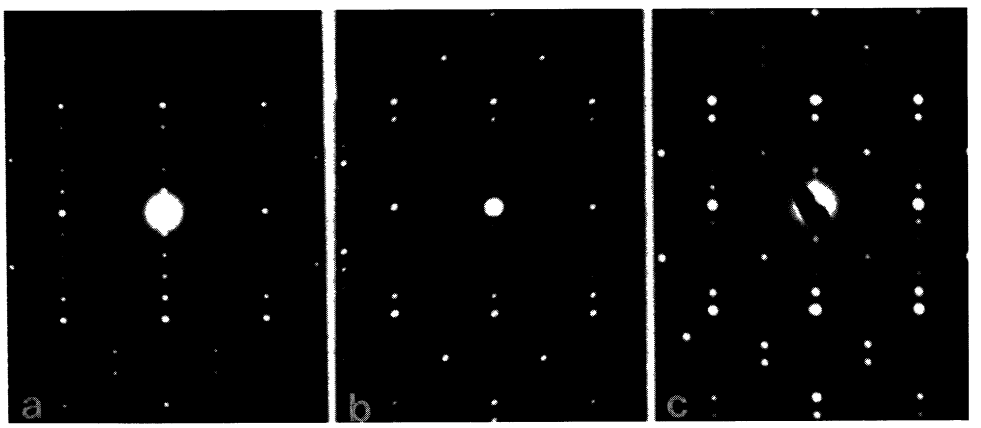

Fig. 5. — ED-patterns in [001] projection of a) $U(Mo, W)_4O_{14}$; b)$U_{0.5}$ $(Mo, W)_{11}O_{34}$; c)$U(Mo, W)_5O_{17}$.

The micrograph of the first phase (Fig. 6a) shows that the ReO_3–type slabs are four MO_6–octahedra wide. From an X-ray powder pattern the unit cell dimensions were found to be $a = 35.007$ Å, $b = 7.3610$ Å and $c = 4.0562$ Å. The single crystal X-ray investigation yielded the structure model in figure 6b. The structure can be described as built up of ReO_3–type slabs four octahedra wide and linked by U- and O-atoms so that a pleated edgesharing arrangement of pentagonal UO_7-bipyramids is formed.

The HREM image in figure 7a shows an ordered crystal fragment. The corresponding ED pattern is identical to that shown in figure 5b. The square array of black spots represents corner-sharing MO_6–octahedra in ReO_3–type slabs. The micrograph clearly shows that the slab width corresponds to five octahedra. The linkage plane between the slabs, which is imaged as an almost

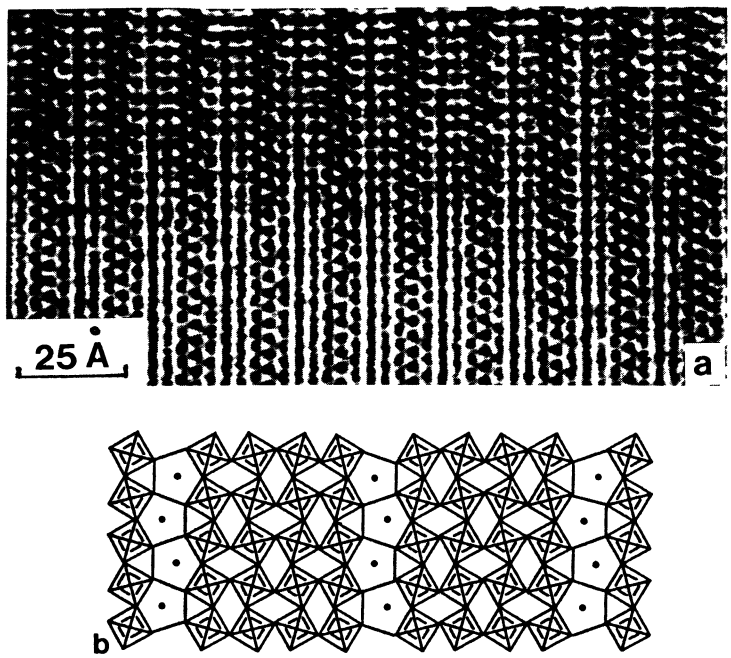

Fig. 6. — a) HREM image of $U(Mo, W)_4O_{14}$. [001] projection, b) Idealized structure model of $U(Mo, W)4O_{14}$.

straight row of black spots, cannot be directly interpreted from the HREM image. However, considering the doubling of the a–axis, which is obvious from the ED pattern in figure 5b, it is most likely that the slabs are linked as in figure 1b. The row of black spots can thus be interpreted as an ordered arrangement of MoO_6–octahedra and hexagonal UO_8–bipyramids. The corresponding structure model, projected along the short c–axis, is shown in figure 7b. This structure is homologous with the $U_{0.5}(Mo, W)_7O_{22}$ phase above; only the widths of the ReO_3–type slabs differ. The composition can be calculated to be $U_{0.5}(Mo, W)_{11}O_{34}$. Charge balance requires that only half of the hexagonal bipyramids formed should be occupied by U atoms The MO_6–octahedra are all assumed to be randomly occupied by Mo and W. From the thinner part of the crystal fragment in figure 7a, it can be seen that the intensity of the black spots along the linkage plane between the ReO_3–type slabs varies. At a few places, marked by arrows, the spots are almost unobservable, which should be due to the presence of uranium vacancies. The U vacancies seem to be randomly distributed in the structure, however, as no indications of streaking or superstructure reflexions have been observed so far. EDS-analysis of a few fragments with identical ED-patterns, as in figure 5b, indicate a low uranium content. The EDS- results so far obtained are all in agreement with the calculated composition, and they show that the most likely composition is close to $U_{0.5}Mo_3W_8O_{34} = U_{0.5}(Mo, W)_{11}O_{34}$. No crystal of the $U_{0.5}(Mo, W)_{11}O_{34}$ phase, suitable for single-crystal x-ray studies, has so far been found.

EDS-analysis of fragments giving the ED-pattern shown in figure 5c, indicated a much higher uranium content than that of the $U_{0.5}(Mo, W)_{11}O_{34}$ phase. The composition of the fragment is closer to $U(Mo, W)_5O_{17}$.

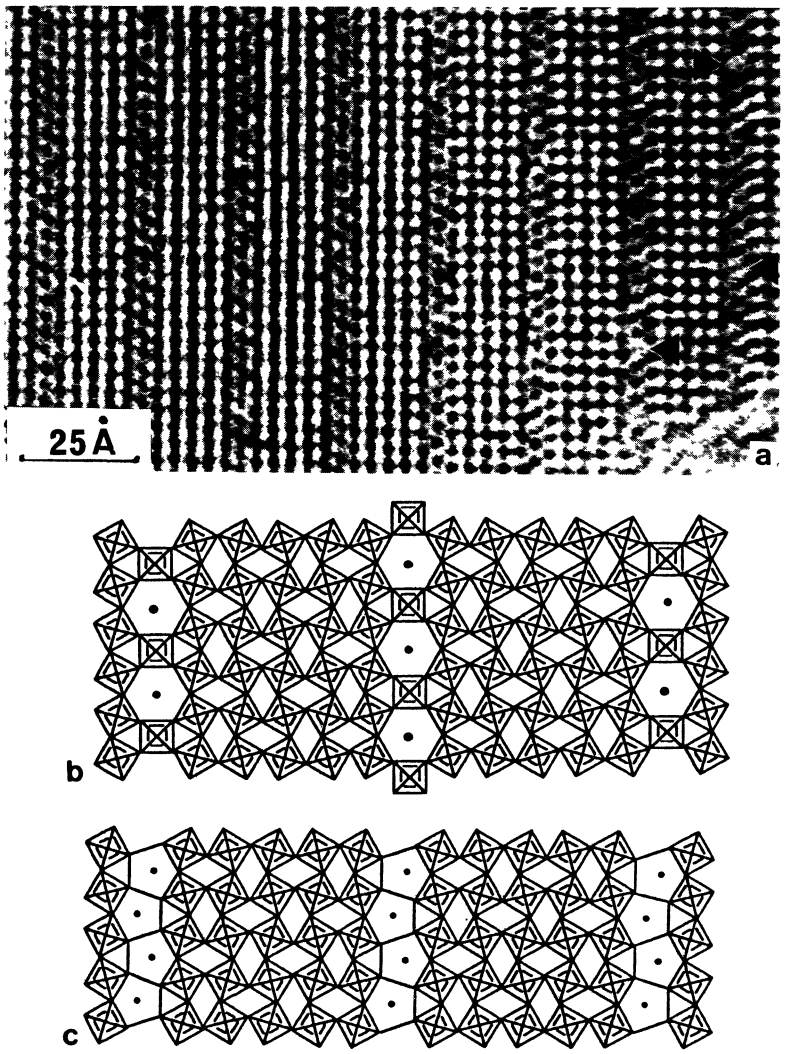

Fig. 7. — a) HREM image of a thin fragment of $U_{0.5}(Mo, W)_{11}O_{34}$, arrows mark almost empty six-sided tunnels. b) Idealized structure model of $U_{0.5}(Mo, W)_{11}O_{34}$. c) Idealized structure model of $U(Mo, W)_5O_{17}$.

d) $U(Mo, W)_5O_{17}$.

X-ray diffraction data were collected from a single crystal selected from the UO_2 : MoO_3 : WO_3 =1:1:13 sample. The structure determination resulted in the model shown in figure 7c. From x-ray powder data the unit cell parameters were found to be a =42.484 Å, b =7.3823 Å and c =4.0363 Å. The structure is related to that obtained for the $U_{0.5}(Mo, W)_{11}O_{34}$ phase above. Both structures contain slabs that are five MO_6–octahedra wide, but the atom arrangements between the slabs are different. In figure 7c, only U- and O-atoms are located between the slabs in such a way that a pleated, edgesharing chain of pentagonal UO_7–bipyramids is formed, identi-

cal to that previously observed in the $\beta - UMo_2O_8$ structure (Fig. 1a). The single-crystal X-ray results strongly support this arrangement. The unit cell content in figure 7c corresponds to the stoichiometric formula $U(Mo, W)_5O_{17}$. All U-atom positions in the linkage plane are fully occupied by U-atoms. The X-ray study also showed a puckered arrangement of the metal atoms. The displacement, $\pm\Delta z$, of M-atoms from the $z = 0$ plane in the ReO_3–type slabs doubles the a-axis.

Some of the selected crystals were also used for electron microscopy study. All electron diffraction patterns recorded were identical to that shown in figure 5c, with cell dimensions $a \approx 21.4$ Å and $b \approx 7.4$ Å. Because of systematic $hk0$ absences, the periodicity along a shows up as half of the actual value. EDS-analysis of twenty fragments, indicated that a likely composition is close to $UMo_{0.8}W_{4.2}O_{17}$.

The EDS-analysis in combination with the corresponding electron diffraction study and the x-ray results, showed that two different, but closely related phases exist, viz. $U(Mo, W)_5O_{17}$ and $U_{0.5}(Mo, W)_{11}O_{34}$. One phase has a slightly higher uranium content than the other, but they have almost identical unit cell dimensions.

e) $U_{0.5}(Mo, W)_9O_{28}$.

The last example illustrates ordered vacancies. Electron diffraction patterns of selected crystals from the bulk sample $UO_2 : MoO_3 : WO_3 = 1:3:8$ were similar to the patterns shown in figure 5. Figure 8a illustrates that weak superstructure reflexion spots doubles both the a– and c–axes of the unit cell.

The unit cell parameters obtained from figure 8a are $a \approx 2\times 17.6 \approx 35.2$ Å and $b \approx 2\times 7.2 \approx 14.4$ Å. The micrograph in figure 8b shows that the ReO_3–type slabs are four octahedra in width, and large white spots can be seen regularly distributed (three black spots, one white spot) along the connection planes between the slabs. At a few places, disorder can be observed. The dimensions of the subcell ($a_{sub} \approx 17.6$ Å and $b_{sub} \approx 7.2$ Å) and the contrast features in the HREM images indicate a basic framework structure: a network of cornersharing MO_6–octahedra arranged so that six-sided tunnel are formed, and every second tunnel is filled with -O-U-O-U-O- strings as in figure 8c. The weak superstructure reflexion spots observed in the ED-pattern are caused by ordering of the filled tunnels. The white spots in figure 8b correspond to empty tunnels. The composition of the structure model in figure 8c is $U_{0.5}(Mo, W)_9O_{28}$.

4. Discussion.

The results obtained above are summarized in table I. The structures can be considered as belonging to two homologous series of phases, both built up of ReO_3– type slabs of variable width, but with the slabs mutually connected in different ways.

The structures denotes (n)– PB in table I can be ascribed to a homologous series with the general formula $UO \cdot M_nO_{3n+1}$, where n represents the number of MO_6– octahedra across the ReO_3–type slab. The slabs are interleaved with -U-O-U-O- atom rows so that chains of edgesharing pentagonal UO_7–bipyramids (PB=pentagonal bipyramid) are formed. All uranium positions are fully occupied by uranium atoms. The $UMoO_5$ phase, which is isostructural with UVO_5 [11], is the first member ($n = 1$) of this series and will thus be denoted (1)-PB, while the $\beta - UMo_2O_8$ phase corresponds to (2)-PB. For the members (4)-PB and (5)-PB described above, the Mo-atoms have to a large extent been replaced by W-atoms. Alternatively, this set of structures can be considered as intergrowths of UVO_5– and ReO_3– type structure elements.

The other class of structures observed so far in the examined subsystems, denoted (n)–HB in

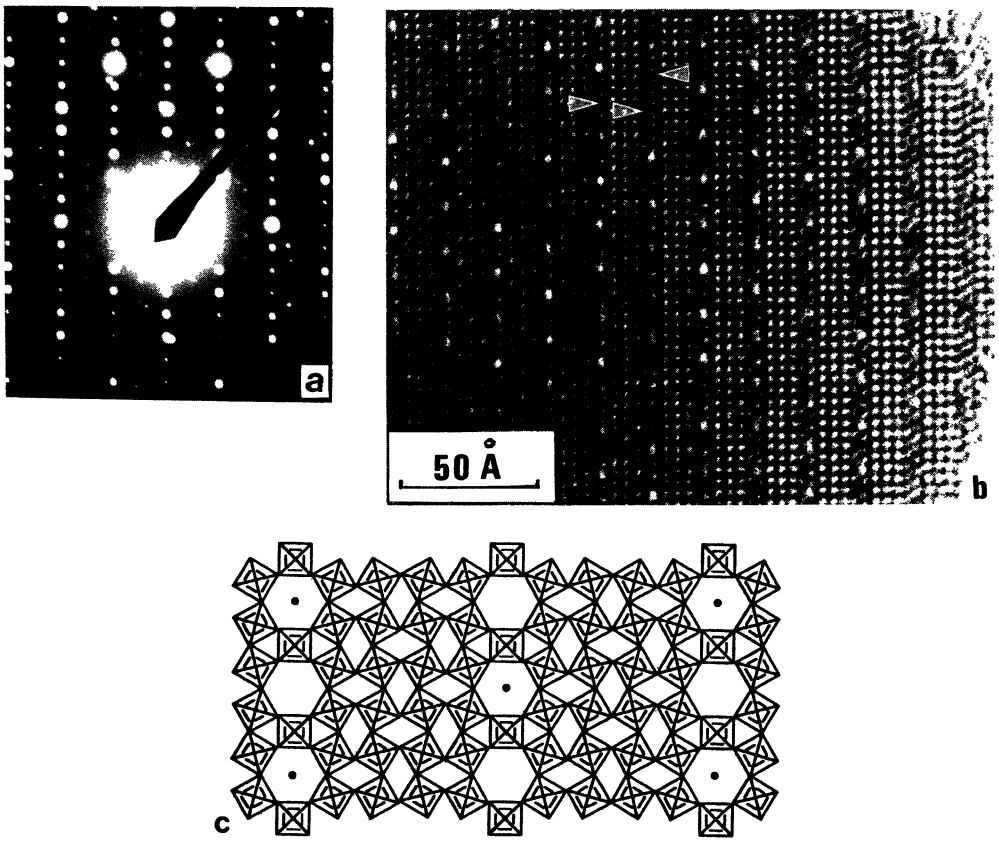

Fig. 8. — a) ED-pattern, [001] projection, of $U_{0.5}(Mo, W)_9O_{28}$. b) Corresponding micrograph of a thin crystal fragment. Arrows mark disorder in the filling of the six-sided tunnels. c) Idealized structure model of $U_{0.5}(Mo, W)_9O_{28}$.

Table I.

Compound	Number of octahedra in the ReO_3–type slab (n)	Coordination of U – atom	Occupancy of U in bipyramids	Denotation of structure	References
$UMoO_5$	1	7	1.0	(1) – PB	[11]
$\beta - UMo_2O_8$	2	7	1.0	(2) – PB	[7]
$U(Mo, W)_4O_{14}$	4	7	1.0	(4) – PB	This study, [8]
$U(Mo, W)_5O_{17}$	5	7	1.0	(5) – PB	This study, [8]
UMo_5O_{16}	2	8	1.0	(2) – HB	This study
$\alpha - U_3Mo_{20}O_{64}$	2	8	0.75	(2) – HB	[4]
$UMo_{10}O_{32}$	2	8	0.50	(2) – HB	[5]
$U_{0.5}(Mo, W)_7O_{22}$	3	8	0.50	(3) – HB	This study
$U_{0.5}(Mo, W)_9O_{28}$	4	8	0.50	(4) – HB	This study
$U_{0.5}(Mo, W)_{11}O_{34}$	5	8	0.50	(5) – HB	This study

table I, can be considered as a homologous series with the general formula $U_{1-x}\,\square_x\,O \cdot mMO_3$ (□=vacancy), with $m = 2n + 1$, where n is the number of octahedra across the ReO_3–type slab. The structures can be described as built up of a basic network of cornersharing MO_6–octahedra arranged so as to form slabs of six-sided tunnels separated by ReO_3–type slabs of width n. The former slabs are HTB (hexagonal tungsten bronze) elements one tunnel row wide. Thus, the basic structure can be regarded as an intergrowth between slabs of HTB-type and ReO_3–type structures. Chains of -O-U-O-U-O- enter the six-sided tunnels and thus transform them to chains of cornersharing hexagonal UO_8–bipyramids (HB=hexagonal bipyramids), running along the short crystal axis. In the UMo_5O_{16} ($UO \cdot 5MoO_3$) structure, all uranium atom positions are fully occupied ($x = 0$), while in the $\alpha - U_3Mo_{20}O_{64}$ structure ($x = 0.25$) 25% of the uranium positions are vacant. The formula $\alpha - U_3Mo_{20}O_{64}$ can thus be rewritten as $\alpha - U_{0.75}\,\square_{0.25}\,O \cdot 5MoO_3$. Other phases are formed where only half of the uranium atom positions are occupied ($x = 0.5$). The $UMo_{10}O_{32}$ structure in figure 1b can be formulated as $U_{0.5}\,\square_{0.5}\,O \cdot 5MoO_3$. As can be seen from table I, UMo_5O_{16}, $\alpha - U_3Mo_{20}O_{64}$ and $UMo_{10}O_{32}$ are all denoted (2)-HB, since their basic framework structures are the same; but they differ in the degree of filling of the hexagonal UO_8–bipyramids. Replacement of molybdenum by tungsten creates larger ReO_3–type slabs. The phases with n =3, 4 and 5 have been reported above. The (4)-HB structure contained ordered vacancies. The creation of randomly distributed vacancies in the structure might indicate that UO_2–groups are formed in the structures. An average uranium content in the hexagonal bipyramids, $x < 0.5$, have not so far been observed. This might also indicate that $(O - U - O)^{2+}$ -groups should be present in the examined phases.

All structure models clearly show that the ReO_3–type slabs consist of tilted octahedra. In the homologous series $UO \cdot M_nO_{3n+1}$, $((n) - PB)$, members with n = odd have a cell with the a–axis doubled, whereas the doubling is seen for n =even in the other homologous series $U_{1-x}\,\square_x\,O \cdot mMO_3\,((n) - HB)$. In the latter case, because of the tilt of the octahedra, the six-sided tunnels in two adjacent rows will be at the same y level if there is an even number of octahedra between the rows, as in the UMo_5O_{16}. (2)-HB, and $U_{0.5}\,(Mo, W)_9O_{28}$, (4)-HB, structures. On the other hand, two adjacent rows with six-sided tunnels will be displaced by Δy =1/2 relative to each other, if there is an odd number in the ReO_3–type slabs, as in $U_{0.5}(Mo, W)_7O_{22}$, (3)-HB, and $U_{0.5}(Mo, W)_{11}O_{34}$, (5)-HB.

Intergrowth between structures of the two homologous series $UO \cdot M_nO_{3n+1}$ $((n) - PB)$ and $U_{1-x}\,\square_x\,O \cdot mMO_3((n) - HB)$, modelled in figure 9, might easily occur. Theoretical image calculations have shown that such intergrowth would be difficult to observe in HREM images of thin regions. However, it seems likely that this might occur as local defects. Such local defects would have only a minor influence on the total composition.

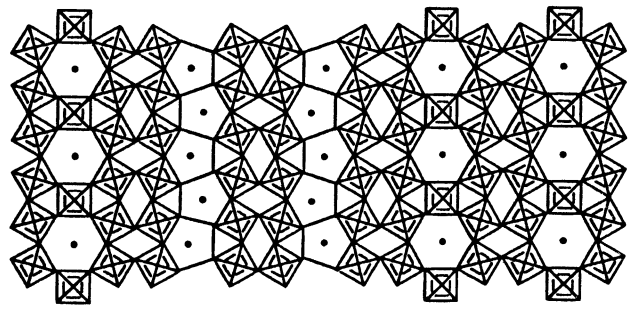

Fig. 9. — Idealized structure model showing hypothetical intergrowth of the UMo_5O_{16} and $\beta - UMo_2O_8$ structures.

When the basic structure of the $U_{1-x}\,\square_x\,O \cdot mMO_3$ family of homologous phases is considered as an intergrowth between slabs of HTB-elements, one tunnel row wide, and the ReO_3–type structure, then the resemblance to the intergrowth tungsten bronzes (ITB) [12] is obvious. In the ITB bronzes, alkali atoms enter the six-sided tunnels while in the uranium compounds -U-O-U-O- strings enter the tunnels and thus transform them into cornersharing hexagonal UO_8–bipyramids. ITB bronze structures, where slabs of HTB-elements that are just one tunnel row wide are intergrown with ReO_3–type regions, have been observed in a few samples with low alkali content e.g. $Cs_{0.03}WO_3$ and $Cs_{0.05}WO_3$ [12,13] and also in $Ba_{0.04}WO_3$, $Pb_{0.04}WO_3$ and $Sn_{0.04}WO_3$ [14]. The ReO_3–type slabs are wider for the ITB-bronzes (7-11 octahedra in the slabs) than for the related uranium phases presented above. For the ITB bronzes, intergrowth between various members of the homologous series occur frequently.

The ED-patterns of the $U(Mo, W)_4O_{14}$ and $U(Mo, W)_5O_{17}$ phases shown in figure 5a and 5c are similar to those previously published for UW_4O_{14} and UW_5O_{17} (8). Our single-crystal x-ray results given above for the $U(Mo, W)_5O_{17}$ structure have confirmed the suggestion by Zakharov *et al.* that the "tungsten" atoms are shifted from the centre of the octahedra to form puckered layers, causing a doubling of the unit cell. However, it seems likely that some of the W-atoms in the UW_4O_{14} and UW_5O_{17} crystals studied by Zakharov *et al.* might have been replaced by Mo-atoms, since they were taken from a multiphasic sample of composition $UMoW_{13}O_{44}$.

Acknowledgements.

We wish to express our thanks to Professor L. Kihlborg for valuable comments on the manuscript. V.T. acknowlegdes fellowship from the Swedish Institute. Thanks are also due to Mr. Mats Sundberg for valuable help with drawing of the idealized structure models. This investigation has been financially supported by the Swedish Natural Science Research Council.

References

[1] KOVBA L.M. and TRUNOV V.K., *Radiokhimiya* **7** (1964) 316; Engl. trans. *Radiochemistry USSR Jerusalem* **7** (1964) 314.
[2] PAILLERET P., *C.R.Acad. Sci.* **265** (1967) 85.
[3] KOVBA L.M., *Radiokhimiya* **13** (1971) 909; Engl. trans: *Radiochemistry USSR Jerusalem* **13** (1971) 940.
[4] SEREZHKIN V.N., KOVBA L.M. and TRUNOV V.K., *Kristallografiya* **18** (1973) 961.
[5] SEREZHKIN V.N., KOVBA L.M. and TRUNOV V.K., *Kristallografiya* **19** (1974) 379.
[6] SEREZHKIN V.N., RONAMI G.N., KOVBA L.M. and TRUNOV V.K., *J. Inorg. Chem. (Russ.)* **19** (1974) 1036.
[7] CREMERS T.L., ELLER P.G., PENNEMAN R.A. and HERRICK C.C., *Acta Cryst.* **C39** (1983) 1163.
[8] ZAKHAROV N.D., GRIBELUK M.A., VAINSHTEIN B.K., ROZANOVA O.N., UCHIDA K. and HORIUCHI S., *Acta Cryst.* **B39** (1983) 575.
[9] ZAKHAROV N.D., GRIBELUK M.A., VAINSTEIN B.K., KOVBA L.M. and HORIUCHI S., *Acta Cryst.* **A44** (1988) 821.
[10] O'KEEFE M., BUSECK P.R. and IIJIMA S., *Nature (London)* **274** (1978) 322.
[11] CHEVALIER R. and GASPERIN M., *Bull. Soc. Fr. Minéral Crist.* **93** (1970) 18.
[12] HUSSAIN A. and KIHLBORG L., *Acta Cryst.* **A32** (1976) 551.
[13] KIHLBORG L., *Chem. Scr.* **14** (1978-79) 187.
[14] DOBSON M.M., HUTCHISON J.L., TILLEY R.J.D. and WATTS K.A., *J. Solid State Chem.* **71** (1987) 47.